https://doi.org/10.5194/se-2019-131
Preprint. Discussion started: 3 September 2019

Solid Earth
Discussions
Open Access
EGU

Soil-landscape relationship in sandstone-gneiss topolithosequence in Amazonas, Brazil

Julimar da Silva Fonseca[1], Milton César Costa Campos[1], Elilson Gomes de Brito Filho[1]*, Bruno Campos Mantovanelli[2], Laércio Santos Silva[3], Alan Ferreira Leite de Lima[1], José Maurício Da Cunha[1], Emily Lira Simões[1], Luís Antônio Coutrim dos Santos[1]

[1]Universidade Federal do Amazonas - UFAM, Instituto de Educação, Agricultura e Ambiente, Humaitá, Amazonas, Brasil

[2]Universidade Federal de Santa Maria - UFSM, departamento de agronomia, Santa Maria, Rio Grande do Sul, Brasil.

[3]Universidade Estadual Paulista - UNESP, departamento de agronomia, Jaboticabal, São Paulo, Brasil.

*Corresponding author: Elilson Gomes de Brito Filho, Instituto de Educação, Agricultura e Ambiente – Universidade Federal do Amazonas (UFAM), Humaitá, Amazonas, Brasil, Zip code: 69800-000, telephone: +5597981121704, e-mail: bfsambiente@gmail.com.

https://doi.org/10.5194/se-2019-131
Preprint. Discussion started: 3 September 2019

Solid Earth Discussions

1 Abstrac

Soil position in the landscape reveals its history of formation and genesis. Therefore, the landscape is the combination of features of the surface of the earth with subsurface components (parent material), while the soil is a three-dimensional, dynamic natural body inserted in the landscape. This research aimed to study the soil-landscape relationship in a sandstone-gneiss topolithosequence in Amazonas, Brazil. The study was carried out along a 9.253-meter transect from the top downwards the softer slope. Soil profiles were selected in five landscape compartments (top, upper third, lower third, transport foothill, and deposition foothill). Morphological, mineralogical, physical, chemical, and ray diffraction characterizations were performed. Soils had different morphological, physical, chemical, and mineralogical attributes due to the variations of the geological substrate and landscape position. The mineralogy of the clay fraction is composed of kaolinite, goethite, hematite, and gibbsite, with goethite being the predominant iron oxide. A sand fraction dominance was observed in relation to the other fractions in all the profiles, being related to the alluvial nature of the parent material, with the highest values occurring in the lower third. The separation of the landscape into geomorphic surfaces and identification of the parent material were effective for understanding the variation of soil attributes along the landscape.

2 Introductio

The soil is the product of the combinations of factors and processes of formation governed by the local conditions of its occurrence. The intensity of these factors and processes promote progressive transformations in the parent material, which over time are expressed by morphological, chemical, physical, and mineralogical soil properties. Thus, considering the Amazonian environments, climate conditions of high temperature and high precipitation prevail in the Brazilian Amazon, favoring an intense mineral weathering and, therefore, the formation of soils with predominant characteristics (Dalamerlinda et al., 2017). For this reason, it is necessary to recognize the interaction among these factors and their role in soil formation (Campos et al., 2012a; Silva, 2016).

Soil position in the landscape reveals its history of formation and genesis (Campos et al., 2011). Thus, the landscape is the combination of features of the surface of the earth with subsurface components (parent material), while the soil is a three-dimensional, dynamic natural body inserted in the landscape (Minasny and Mcbratney, 2006). In general, soil attributes present the characteristics of the matrix rock, but at a local scale,

https://doi.org/10.5194/se-2019-131
Preprint. Discussion started: 3 September 2019

the occurrence of attributes can be very different due to the existence of more lithologic substrate or even the predominance of a specific formation process (Campos et al., 2012a). Thus, the relief, although considered a supporting factor, acts on the spatial distribution of soil attributes, water dynamics, presence of unconsolidated sediments, pedogenetic development, and processes that translate into the most varied soil types (Bockheim et al., 2005; Vasconcelos et al., 2012; LI et al., 2015).

For a better understanding of the soils in the landscape, the preconized concepts of the soil-landscape relationship become necessary as criteria for understanding the spatiotemporal variability of soil attributes and visualization of dynamic processes such as the transport of water, solutes, and sediments (Sommer, 2006; Campos et al., 2011). Despite the great representation of the Middle Madeira River region, the most common physiographic environments are floodplains, native fields, and transition areas, which are dominated by Inceptisols, Ultisols, and Entisols, thus showing the main characteristic of the Amazon region as a function of the exuberant grouping of landscapes associated with different soil classes in a short space of geographical position (Campos et al., 2012a; Campos et al., 2012b).

The direct effects of the composition of the parent material have been studied in the literature. Montanari et al. (2010) found the dominance of goethite and kaolinite in a concave landform in relation to linear and convex landforms, while the highest hematite contents occurred in linear landforms. Curi and Franzmeier (1984) studied a toposequence of Oxisols and found higher gibbsite concentration in the highest landscape position and kaolinite in the lowest positions associated with goethites of lower mean crystal diameter. All these investigations reinforce the importance of characterizing soil mineralogy to reinforce the relationship between the landscape and parent material, especially Fe and Al oxides because their formation is influenced by environmental conditions and persist for a long time in the soil (Kämpf and Curi, 2000).

Despite the long territorial extension of the Amazon region, studies have been conducted and various characteristics and peculiarities of its landscape have revealed new directions in studies on the soil-landscape relationship. Thus, the properties of the soil-landscape relationship associated with the behavior of parent material transmit records of the intensity of pedogenetic processing conditions that prevailed in the environment that influenced the formation of these soils. Therefore, this research aimed to study the soil-landscape relationship in a sandstone-gneiss topolithosequence in mazonas, Brazil.

3 Material and methods

https://doi.org/10.5194/se-2019-131
Preprint. Discussion started: 3 September 2019

Solid Earth
Discussions
Open Access
EGU

3.1 Characterization of the physical environment

The study area is located at BR 230 km 150 – Transamazônica, municipality of Manicoré, AM – direction of Machadinho do Oeste, RO, at Rodovia do Estanho km 14, located between the geographical coordinates 08°08′12.6″ S and 61°50′06.5″ W (Figure 1). According to the Köppen classification, the regional climate is classified as Am, i.e. a rainy tropical climate (monsoon rains), with a dry period of short duration, temperatures varying from 25 to 27 °C, and annual precipitation of 2,500 mm with the rainy season beginning in October and extending until June and relative air humidity between 85 and 90%.

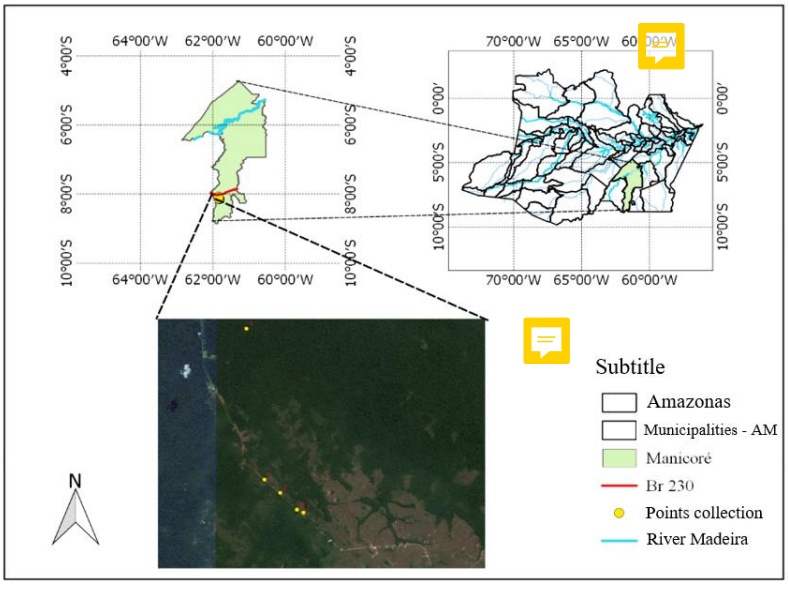

Figure 1. Location of the profiles studied in the municipality of Manicoré in the state of Amazonas, Brazil. Source: ©Google Maps.

Relief configuration is marked by the presence of plateaus in the highest parts, which exhibit flat topographic surfaces, with the border area marked by aligned hills and ridges, while the lower areas constitute a pediplanated surface, locally interrupted by flat top hills (CPRM, 2001).

Regarding the geology, the study area is located on Rondonian Granites characterized by the presence of muscovite, biotite, adamelites, and granodiorites of intrusive cratogenic origin, in the form of stocks and batholiths (BRASIL, 1978). According to ZEE (2008), regional soils are Oxisols. The characteristic vegetation of this region is a dense tropical forest consisting of densified and multi-layered trees between 20 and 50 meters in height (figure 2).

https://doi.org/10.5194/se-2019-131
Preprint. Discussion started: 3 September 2019

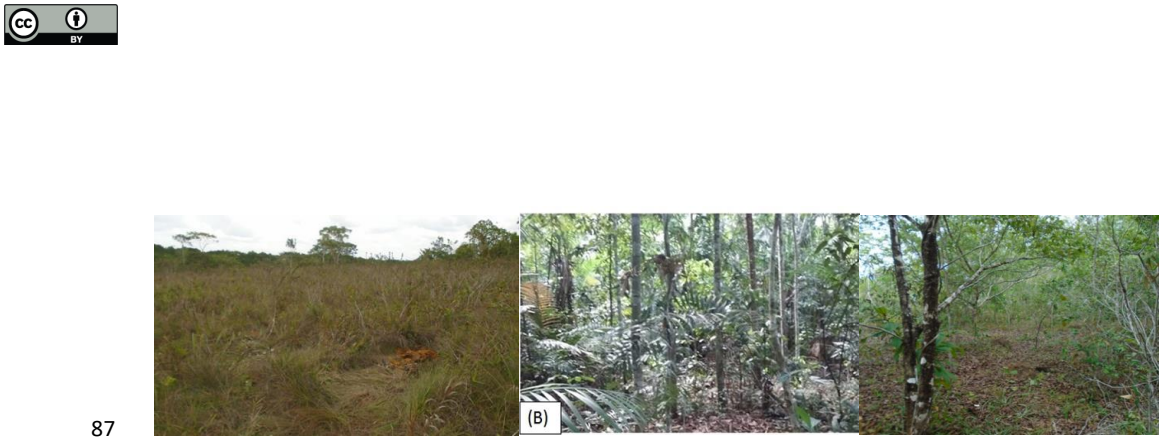

Figure 2. Images of the collection environment.

3.2 Field methodology

The study was carried out along a 9.253-meter transect from the top downwards the softer slope to the deposition foothill. Measurements of the altitudes were carried out along this transect to make the altimetric profile. Based on the model of Dalrymple et al. (1968), hillside segments were identified mainly based on the variation of the terrain slope (Figure 3).

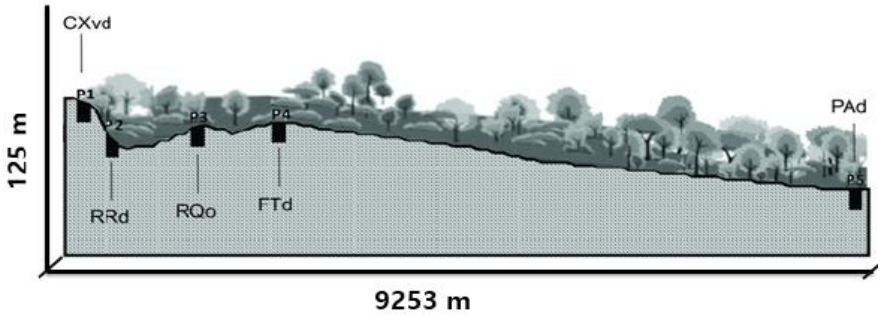

Figure 3. Schematic profile of the terrain topography and trench position in the topolithosequence in Amazonas, Brazil.

Five trenches were opened along the hillside topography following the transect illustrated in Figure 3 in order to characterize the soils, as follows: top (08°08′46.0″ S and 61°49′25.1″ W), upper third (08°08′41.8″ S and 61°49′33.9″ W), lower third (08°08′18.3″ S and 61°49′56.3″ W), transport foothill (08°07′59.6″ S and 61°50′17.4″ W), and deposition foothill (08°07′59.6″ S and 61°50′17.4″ W). The identification of horizons and morphological description, followed by the sampling of soil horizons, were performed according to Santos et al. (2013). Soils were classified according to criteria established by the Brazilian Soil Classification System (Santos et al., 2013).

Twenty samples were collected at different soil profiles: Top: A – 0.0–0.16 m and AB – 0.16–0.30 m; upper third: A – 0.0–0.12 m and ACr – 0.10–0.20 m; lower third: A – 0.0–0.7 m and C1 – 0.15–0.33 m; transport

https://doi.org/10.5194/se-2019-131
Preprint. Discussion started: 3 September 2019

foothill: A – 0.0–0.18 m and AB – 0.18–0.33 m; and deposition foothill: A – 0.0–0.18 m and AB – 0.18–0.32 m. The criterion for choosing the depths was the coincidence with surface and subsurface diagnostic horizons.

3.3 Particle size analysis

Particle size analysis was performed by the pipette method using a 0.1 mol L^{-1} NaOH solution as a chemical dispersant and mechanical stirring in a low rotation apparatus for 16 h (Donagema et al., 2017). The clay fraction was separated by gravitational sedimentation, the coarse and fine sand fraction by sieving, and the silt fraction was calculated by difference.

3.4 Chemical analysis

Soil pH was determined in water and 1.0 mol L^{-1} KCl solution in the soil to solution ratio of 1:2.5 (Donagema et al., 2017). The exchangeable cations Ca^{2+}, Mg^{2+}, and Al^{3+} were extracted with 1.0 mol L^{-1} KCl and measured by atomic absorption spectroscopy. The hydrogen ion and Al^{3+} were extracted with 0.5 mol L^{-1} calcium acetate at pH 7.0 and determined by titration (0.025 mol L^{-1} NaOH) (Donagema et al., 2017). Organic carbon was determined by the wet oxidation method (Walkley and Black, 1934).

Bioavailable particulate phosphorus (Pbp) was determined by extraction with anion exchange resin (AER). The principle of phosphorus extraction by AER is its continuous removal from the solution by the exchange with bicarbonate of the resin, creating a concentration gradient that forces the exit of the surface of colloids until an electrochemical equilibrium is reached between the soil and AER (Skogley and Dobermann, 1996). For this, the methodology developed by Kroth (1998) was used as follows: 0.5 g of soil (1 mm) was added in 15 mL falcon tubes containing 10 mL distilled water and a sheet of AER saturated with 0.5 mol L^{-1} $NaHCO_3$. These tubes were stirred for 16 hours on an end-over-end stirrer (33 rpm). The sheets were removed and washed with distilled water jets and then diluted in 10 mL 0.5 mol L^{-1} HCl. The tubes remained uncapped for 90 minutes and then closed and stirred for 30 minutes in a horizontal stirrer. Subsequently, a 3 mL aliquot was taken from the extract to determine the P content according to Murphy and Riley (1962). The sum of bases (SB), cation exchange capacity (CEC), base saturation (V), and aluminum saturation (m) were calculated based on the results of the chemical analyses.

3.5 Mineralogical analysis

The minerals of the clay fraction hematite (Hm), goethite (Gt), kaolinite (Kt), and gibbsite (Gb) were characterized by X-ray diffractometry using the powder method after the concentration of iron oxides by

https://doi.org/10.5194/se-2019-131
Preprint. Discussion started: 3 September 2019

boiling the clay fraction in NaOH (Norrish and Taylor, 1961) and deferrifying it by the method of Mehra and Jackson (1960). The samples were diffracted with scanning speed of 1° 2θ min^{-1} using a Mini-Flex Rigaku II (20 mA, 30 kV) equipped with Cu Kα radiation. The Hm/(Gt+ Hm) ratio was estimated by comparing the peak areas from the Hm/(Gt+Hm) with the proportions of relationships obtained from standard Gt–Hm mixtures.

The percentages of Hm and Gt were calculated by allocating the difference between Fed and Feo to these oxides. The Kt/(Kt+Gb) ratio was calculated by peak areas of Gb (002) and Kt (001) reflections. The calculation of the content of isomorphic substitution of iron by aluminum in Gt was obtained by the equation mol mol^{-1} = 1730 − 572 c (Schulze, 1984). For the calculation of the content of isomorphic substitution of iron by aluminum in Hm, the equation mol mol^{-1} = 3098.8 − 615.12 a0 (Schwertmann et al., 1989) was used. The specific surface area (SSA) of Gt was estimated by the formula SSA (Gt) = $(1049/MCD\ gt\ 100)^{-5}$ ($m^2\ g^{-1}$), according to Schulze and Schwertmann (1984), MCD100 = MCD (110) × 0.42 nm (Kämpf, 1981), and the SSA of Hm was estimated by the formula SSA (Hm) = 2 × (r + h) × d ($m^2\ g^{-1}$), according to (Schwertmann and Kämpf, 1985). The mean crystal diameter (MCD) of Hm and Gt was calculated from the width at half-height (WHH) and the position of mineral reflections using the Scherrer equation (Klug and Alexander, 1974).

4 Results

4.1 Soil distribution in the landscape

A physiognomy formed by plains was observed in this locality due to the minimal variation of relief. This characteristic is typical in Amazonian environments probably because of the gradual transition action that occurs between fields and the forest in this region. The lowest terrain position is colonized by small shrub species, where there are flood conditions at certain times of the year. Dalrymple et al. (1968) established hypothetical units of hillsides, which may be partially absent or repeated along them. In this study, five hillside segments were identified and mapped in a representative toposequence of the region (Figure 3).

The first three hillside segments of the landscape, represented by the top, upper third, and lower third, with elevations from 120 to 125 m, are grouped similarly among each other. This position in the landscape does not confer greater stability to soil attributes, mainly due to the classification of these soils, thus evidencing the total influence of the landscape on its attributes. The third segment is the transport foothill (119 m), with a residual erosional character, starting from the edges of the lower third and showing a slightly sloping conformation to the fifth segment, which may have been formed by relief microvariations of the previous

https://doi.org/10.5194/se-2019-131
Preprint. Discussion started: 3 September 2019

segment. Finally, the fifth segment is the deposition foothill, which presents lower altitudes than the top (between 114 and 116 m), but with different topographic characteristics. In this case, it may be considered a stable geomorphic environment.

The pedogenesis of these soils evidences the action of more than one parent material since the partition is composed of five distinct classes in the different segments. Considering that these classes were developed on different sandstone-gneiss parent materials, they are the main cause of alterations in soil attributes at different magnitudes. As observed by Marques Júnior and Lepsch (2000) and Campos (2012c), understanding the different parent materials in a landscape favor the understanding of the variability of soil attributes, thus indicating that geology provides subsidies to explain the local relief and soil behavior.

4.2 Morphological and textural attributes

The genesis and classification showed that all profiles have a moderate diagnostic surface A horizon (Table 1). The topographic position of the top showed an incipient subsurface diagnostic B horizon, with no evidence of predominant pedogenic process, being classified as a leptic Dystrophic Ta Haplic Cambisol.

Soils of the upper and lower third are poorly evolved, consisting of mineral material or organic material lower than 20 cm thick, with no type of diagnostic B horizon. In the upper third, the soil was characterized as a Regolithic Neosol because it is in a lytic contact at a depth higher than 50 cm and A horizon overlying C or Cr horizon, presenting altered primary minerals, with gravels from the ACr horizon at a depth of 12–35 cm and presence of fragments of semi-weathered rocks (Santos et al., 2013). On the same surface, there was the presence of Quartzarenic Neosol (lower third), soils with no lytic contact within 50 cm of depth, with sequences of A–C horizons, but showing a sand or loamy sand texture in all horizons up to at least 150 cm, mainly consisting of quartz with coarse and fine sand fractions and whitish colors (Santos et al., 2013).

The transport foothill, submitted to a higher influence of seasonal variations of the water table, presented mottles in the subsurface horizons of a reddish color, with a small size and distinct contrast. Associated with the mottled color is the presence of plinthite and petroplinthite in amounts varying from common to abundant, corresponding to values between 15 and 40% of the soil volume. These attributes indicate the occurrence of the plinthization pedogenic process, being a diagnostic character of the plinthic horizon, according to the Brazilian Soil Classification System (SiBCS) (Santos et al., 2013). From the attributes and identified horizons, the profile was classified, at suborder level, as an 3.3 Argiluvic Plinthosol.

https://doi.org/10.5194/se-2019-131
Preprint. Discussion started: 3 September 2019


Solid Earth Discussions

In this segment, there was the presence of an abruptic Dystrophic Yellow Argisol (deposition foothill), presenting textural B horizon and predominance of colors with hue 10 YR and 7.5 YR in the first 100 cm of the B horizon. In this soil, the slope was determinant for the selective removal of clay, contributing to the formation of a textural gradient. In summary, the mineralogical, physical, and chemical results of the characterized profiles accurately elucidated the characteristics of the sandstone-gneiss rock that originated the soils along the topolithosequence.

Soil colors ranged from very dark grayish brown to dark brown in the surface horizons (Table 1). Thus, a clear differentiation was observed for subsurface horizons that have colors from yellowish brown to very pale brown. The grayish tones were observed in most horizons, being this coloration associated with a low concentration of iron oxides and predominance of light-colored minerals such as kaolinite and quartz in the sand fraction (EMBRAPA, 2013). This behavior can be verified in Table 3, which shows the predominance of goethite in all profiles, even in the Plinthosol, which showed higher increases of hematite.

Surface horizons had the predominance of a weak, small, medium to large structure in the composition of the top and foothill (Table 1). On the other hand, in transport and deposition foothills predominated a moderate, medium, coarse to large structure. According to Silva et al. (2001), the soil drainage, conditioned by the topographic position, has a strong relationship with the type of structure because moderately to well-drained soils tend to have granular or angular and subangular blocky structures, while poorly to imperfectly drained soils tend to exhibit a standard structure in polygonal prisms. Campos et al. (2012a) observed that the relief conditions influenced several soil attributes, considering that the slope creates a complex pattern of transport of water and solutes, acting mainly on soil profile development.

The surface horizon of all profiles presented a sandy loam textural class, except for Neosols, which presented a sandy constitution (Table 1). The dominance of the sand fraction in the profiles is explained by the parent material, composed of sandstones of the Palmeiral Formation and Nova Campo Verde Complex. However, the increase in the clay fraction in the Argisol from the Bt1–Bt2–Btf horizon stood out. As highlighted by Campos et al. (2011) and verified in our study, Argisol and Plinthosol seem to have undergone a process of rejuvenation due to their position in the landscape, with a probable loss of clay from the surface horizons, resulting in an abrupt textural change.

218 TABLE 1. Morphological and granulometric attributes of a topolithosequence in Amazonas, Brazil.

Horizon	Depth	Color	Texture	Structure	Clay	Silt	Fine sand	Coarse sand	Total sand	S/C
Top – Leptic Dystrophic Ta Haplic Cambisol – CXvd										
A	0–16	10 YR 3/2	Sandy loam	weak, small, granular	128	182	386	304	690	1.43
AB	16–30	10 YR 3/2	Sandy loam	moderate to medium, angular and subangular blocks	132	198	393	277	670	1.50
Bi	30–55	10 YR 4/6	Sandy loam	weak, medium, angular and subangular blocks	139	213	416	232	648	1.53
BCr	55–78+	10 YR 4/4	Sandy loam	weak, small to medium, granular	142	212	422	224	646	1.49
Upper third – Leptic Dystrophic Regolithic Neosol – RRd										
A	0–12	10 YR 3/2	Sandy loam	weak, small, granular	118	141	241	500	741	1.19
ACr	12–35	10 YR 4/6	Sandy loam	weak, small, angular and subangular blocks	111	159	269	460	730	1.43
Cr/Bi	35–62	10 YR 6/6	Sandy loam	weak, small, angular and subangular blocks	116	161	289	441	723	1.33
Lower third – Typic Orthic Quartzarenic Neosol – RQo										
A	0–15	10 YR 3/2	Sand	weak, small to medium, granular	56	53	62	829	891	0.94
C_1	15–33	10 YR 7/2	Sandy loam	weak, large, angular and subangular blocks	50	61	121	768	889	1.21
C_2	33–50	10 YR 7/3	Loamy sand	moderate, medium to large, angular and subangular blocks	49	87	130	734	864	1.78
C_3	50–75	10 YR 7/3	Loamy sand	moderate, medium to large, angular and subangular blocks	59	88	83	770	853	1.49
Cr	75–105$^+$	10 YR 6/4	Loamy sand	moderate, medium to large, angular and subangular blocks	53	98	126	723	849	1.86
Transport foothill – Typic Dystrophic Argiluvic Plinthosol – FTd										
A	0–18	10 YR 2/1	Sandy loam	moderate, medium to large, granular	131	306	413	150	563	2.32
AB	18–33	10 YR 3/2	Sandy loam	weak, medium to large, angular and subangular blocks	146	329	467	58	525	2.26
BAf	33–48	10 YR 4/6	Loam	weak to moderate, small to medium, angular and subangular blocks	205	336	435	24	459	1.64
Bf	48–70	10 YR 5/6	Loam	strong, large, angular and subangular blocks	257	360	362	21	383	1.41
BCr	70–110$^+$	10 YR 6/4	Loam	strong, medium to large, angular and subangular blocks	258	297	432	13	445	1.15
Deposition foothill – Abruptic Dystrophic Yellow Argisol – Pad										
A1	0–18	10 YR 5/6	Sandy loam	weak, small to large, granular	99	146	406	349	755	1.49
A2	18–32	10 YR 5/6	Sandy loam	moderate, medium to large, angular and subangular blocks	99	172	415	314	729	1.73
AB	32–49	10 YR 5/6	Sandy loam	strong, medium to large, angular and subangular blocks	95	205	416	284	700	2.15
Bt_1	49–74	10 YR 6/8	Clay	strong, medium to large, angular and subangular blocks	548	218	188	47	234	0.40
Bt_2	74–110	10 YR 6/4	Clay	strong, large to very large, angular and subangular blocks	558	228	189	26	215	0.41
Btf	110–125	10 YR 6/8	Clay	strong, large to very large, angular and subangular blocks	563	230	202	5	207	0.41

219 S/C: silt to clay ratio.

https://doi.org/10.5194/se-2019-131
Preprint. Discussion started: 3 September 2019

Soils of the upper and lower third are poorly evolved, consisting of mineral material or organic material lower than 20 cm thick, with no type of diagnostic B horizon. In the upper third, the soil was characterized as a Regolithic Neosol because it is in a lytic contact at a depth higher than 50 cm and A horizon overlying C or Cr horizon, presenting altered primary minerals, with gravels from the ACr horizon at a depth of 12–35 cm and presence of fragments of semi-weathered rocks (Santos et al., 2013). On the same surface, there was the presence of Quartzarenic Neosol (lower third), soils with no lytic contact within 50 cm of depth, with sequences of A–C horizons, but showing a sand or loamy sand texture in all horizons up to at least 150 cm, mainly consisting of quartz with coarse and fine sand fractions and whitish colors (Santos et al., 2013).

The transport foothill, submitted to a higher influence of seasonal variations of the water table, presented mottles in the subsurface horizons of a reddish color, with a small size and distinct contrast. Associated with the mottled color is the presence of plinthite and petroplinthite in amounts varying from common to abundant, corresponding to values between 15 and 40% of the soil volume. These attributes indicate the occurrence of the plinthization pedogenic process, being a diagnostic character of the plinthic horizon, according to the Brazilian Soil Classification System (SiBCS) (Santos et al., 2013). From the attributes and identified horizons, the profile was classified, at suborder level, as an 3.3 Argiluvic Plinthosol.

In this segment, there was the presence of an abruptic Dystrophic Yellow Argisol (deposition foothill), presenting textural B horizon and predominance of colors with hue 10 YR and 7.5 YR in the first 100 cm of the B horizon. In this soil, the slope was determinant for the selective removal of clay, contributing to the formation of a textural gradient. In summary, the mineralogical, physical, and chemical results of the characterized profiles accurately elucidated the characteristics of the sandstone-gneiss rock that originated the soils along the topolithosequence.

Soil colors ranged from very dark grayish brown to dark brown in the surface horizons (Table 1). Thus, a clear differentiation was observed for subsurface horizons that have colors from yellowish brown to very pale brown. The grayish tones were observed in most horizons, being this coloration associated with a low concentration of iron oxides and predominance of light-colored minerals such as kaolinite and quartz in the sand fraction (EMBRAPA, 2013). This behavior can be verified in Table 3, which shows the predominance of goethite in all profiles, even in the Plinthosol, which showed higher increases of hematite.

Surface horizons had the predominance of a weak, small, medium to large structure in the composition of the

https://doi.org/10.5194/se-2019-131
Preprint. Discussion started: 3 September 2019


Solid Earth Discussions

top and foothill (Table 1). On the other hand, in transport and deposition foothills predominated a moderate, medium, coarse to large structure. According to Silva et al. (2001), the soil drainage, conditioned by the topographic position, has a strong relationship with the type of structure because moderately to well-drained soils tend to have granular or angular and subangular blocky structures, while poorly to imperfectly drained soils tend to exhibit a standard structure in polygonal prisms. Campos et al. (2012a) observed that the relief conditions influenced several soil attributes, considering that the slope creates a complex pattern of transport of water and solutes, acting mainly on soil profile development.

The surface horizon of all profiles presented a sandy loam textural class, except for Neosols, which presented a sandy constitution (Table 1). The dominance of the sand fraction in the profiles is explained by the parent material, composed of sandstones of the Palmeiral Formation and Nova Campo Verde Complex. However, the increase in the clay fraction in the Argisol from the Bt1–Bt2–Btf horizon stood out. As highlighted by Campos et al. (2011) and verified in our study, Argisol and Plinthosol seem to have undergone a process of rejuvenation due to their position in the landscape, with a probable loss of clay from the surface horizons, resulting in an abrupt textural change.

In general, the profiles of the soil-landscape relationships presented morphological variations among each other, being the result of a variety of pedogenetic factors and processes. Ribeiro et al. (2012) indicated that the morphological characteristics are due to the soil constitution and conditions under which it was formed, allowing making inferences on pedogenetic processes and environmental conditions, as well as interpreting or predicting the plant behavior and the response of management practices.

Particle size composition showed a predominance of the sand fraction over the other fractions, with contents from 207 and 891 g kg^{-1} (Table 1). These characteristics can be explained by the parent material (sandstone), which presented in their constitution predominance of quartz. These high values of total sand are in accordance with Schiavo et al. (2010), who characterized and classified soils developed from sandstones of the Aquidauana Formation.

In the A horizon, silt contents ranged from 53 to 306 g kg^{-1}, with an increment in depth (Table 1). Low values are associated with young soils still in the formation process. In fact, because they are formed from alluvial sediments, a particle selection may have occurred, leaving in the soil lithogenic (more resistant to changes) and pedogenic materials (with a higher degree of crystallinity). Unlike the sand fraction, the clay fraction

https://doi.org/10.5194/se-2019-131
Preprint. Discussion started: 3 September 2019

increased gradually with depth, with values from 48 to 558 g kg^{-1}. However, we cannot say this is a pedogenic process of eluviation and illuviation. The most likely is the selective removal of surface horizons (more sandy), with clay accumulation in the subsurface.

Neosols presented higher proportions of coarse fractions (> 2 mm) of consolidated ferruginous material as plinthite and petroplinthite due to a possible lowering of the water table, leading to a better drainage of the environment, which was confirmed by the presence of a more reddish hue (2.5 YR) in relation to the other profiles from 48 cm from the surface (Table 1). This predominance of coarser sand fractions, together with the marked presence of gravels, are indicative characteristics that the weathering processes in this soil were not able to promote a marked fragmentation of these fractions (EMBRAPA, 2013).

In the transport foothill, the clay contents ranged from 95 to 99 g kg^{-1} in the A, AB, and BA horizons to 548 g kg^{-1} in the Bt1 horizon, 558 g kg^{-1} in the Bt2 horizon, and 567 g kg^{-1} in the Btf horizon. The marked textural differentiation between the A and Bt1 horizons characterizes an abrupt textural change with a significant increase of clay in relation to the overlying horizons (Table 1).

At the top and upper and lower thirds, the silt to clay ratio (S/C) ranged from 1.43 to 1.50 and 1.19 to 1.43, respectively (Table 1), being associated with less developed soils. The transport foothill showed the lowest S/C ratio, with values between 0.7 and 0.8. On the contrary, the deposition foothill presented the highest values (1.49) in the surface horizons but decreasing to 0.41 with variations in depth. According to Campos et al. (2011), higher values of S/C ratio are due to the low increase in the silt fraction or clay loss, suggesting that small relief variations provide relative losses or gains and, possibly, are not motivated by variations in the parent material.

Considering the topographic variations, clay and silt contents tended to increase towards the youngest geomorphic surfaces, i.e. from the top and thirds to the transport and deposition foothills, in an opposite direction to that of the total sand, which reflects their recent sedimentary nature since the soils of these geomorphic environments are closely related to the parent material. Campos et al. (2012b) also evidenced this condition when studying the soil-geomorphic surface relationships in a toposequence floodplain-upland in the region of Humaitá, AM, Brazil.

4.3 Variation of chemical attributes

The values of pH ranged from 4.17 to 5.48 (H_2O) and 3.81 to 5.70 (KCl), especially in the upper and lower

https://doi.org/10.5194/se-2019-131
Preprint. Discussion started: 3 September 2019

304 thirds and deposition foothill, presenting the highest acidity content in the surface horizon. According to
305 Campos et al. (2012b), the high regional precipitation contributes significantly to base leaching, increasing
306 soil pH. The balance of negative net charges, expressed by ΔpH in the B horizon, showed the highest values
307 at the top and upper and lower thirds, which is in accordance with the trend of occurring soils with a lower
308 degree of evolution in the youngest surface (Table 2).

309 TABLE 2. Soil chemical attributes in a topolithosequence in Amazonas, Brazil.

Horizon	pH		Ca^{2+}	Mg^{2+}	K^{+}	SB	Al^{3+}	H+Al	CEC	m	V	P resin	OC
	H_2O	KCl	- - - - - - - - - - - - - - - -			$cmol_c\ dm^{-3}$		--- -- - - - - -		--%--		$mg\ dm^{-3}$	$g\ kg^{-1}$
Top – Leptic Dystrophic Ta Haplic Cambisol – CXvd													
A	4.79	3.81	1.00	0.15	0.12	1.27	4.3	19.42	21	77	6	4.6	59.33
AB	4.94	4.50	0.20	0.14	0.11	0.35	4.4	19.38	20	93	2	3.1	26.50
Bi	4.62	4.42	0.30	0.09	0.12	0.51	4.9	18.48	19	91	3	2.8	31.49
BCr	5.11	4.34	0.20	0.06	0.070	0.33	4.8	19.32	20	94	2	2.4	15.94
Upper third – Leptic Dystrophic Regolithic Neosol – RRd													
A	4.17	3.89	0.40	0.17	0.11	0.68	5.5	18.21	19	87	4	3.9	47.42
ACr	4.41	4.3	0.20	0.14	0.09	0.43	5.4	16.23	17	91	3	2.7	30.34
Cr/Bi	5.19	4.25	0.30	0.14	0.09	0.53	5.2	14.47	15	89	4	2.8	26.36
Lower third – Typic Orthic Quartzarenic Neosol – RQo													
A	4.91	4.16	0.20	0.12	0.09	0.41	4.3	19.17	20	91	2	2.6	48.19
C_1	5.2	4.70	0.40	0.12	0.06	0.58	5.3	17.25	18	90	3	2.0	34.69
C_2	4.97	4.43	0.40	0.12	0.08	0.60	5.5	15.88	16	90	4	2.1	19.78
C_3	4.72	4.16	0.20	0.12	0.08	0.40	5.7	17.77	18	93	2	2.2	6.34
Cr	4.8	4.13	0.50	0.15	0.10	0.75	5.6	18.21	19	88	4	2.1	0.19
Transport foothill – Typic Dystrophic Argiluvic Plinthosol – FTd													
A	4.95	3.97	0.40	0.17	0.12	0.69	3.9	26.03	27	85	3	3.1	51.07
AB	5.03	4.19	0.20	0.06	0.09	0.34	3.9	23.73	24	92	1	1.9	42.43
BAf	5.2	4.17	0.60	0.17	0.11	0.88	3.1	18.86	20	78	4	1.4	37.63
Bf	5.35	4.42	0.20	0.09	0.06	0.35	3.5	19.43	20	91	2	1.7	32.64
BCr	5.48	4.52	0.30	0.12	0.06	0.48	3.5	18.15	19	88	3	0.7	29.18
Deposition foothill – Abruptic Dystrophic Yellow Argisol – Pad													
A1	4.23	3.88	0.30	0.15	0.13	0.58	4.3	27.72	28	88	2	5.8	69.89
A2	4.33	4.06	0.70	0.12	0.10	0.92	4.3	24.98	26	82	4	3.3	43.39
AB	4.74	4.15	0.20	0.06	0.06	0.32	4.9	18.66	19	94	2	2.0	37.25
Bt_1	4.83	4.22	0.70	0.09	0.07	0.86	4.2	26.5	27	83	3	2.1	31.68
Bt_2	4.8	4.25	0.60	0.17	0.06	0.84	4.6	25.86	27	85	3	2.2	31.49
Btf	4.23	3.88	0.30	0.15	0.13	0.84	4.9	24.73	26	85	3	2.1	10.67

310 SB: sum of bases; CEC: cation exchange capacity; V: base saturation; m: aluminum saturation; OC: organic
311 carbon.

312 The bases Ca^{2+}, Mg^{2+}, and K^{+} presented values ranging from 0.20 to 1.0 $cmol_c\ kg^{-1}$ (Table 2). In general, the
313 magnitude of this variation is small among the landscape positions, which is mainly due to their reduced
314 contents in the minerals constituting the sandstone-gneiss and climate conditions that favor the advanced soil
315 weathering in the region. Moreover, the predominance of oxidic minerals generates positive charges, which,

https://doi.org/10.5194/se-2019-131
Preprint. Discussion started: 3 September 2019

allied with the more sandy texture, provided the loss or movement of these cations to subsurface horizons. This behavior, however, does not apply to K, which remained at higher concentrations near the soil surface. According to Neves et al. (2009), this is a characteristic attributed to the low diffusion power electrostatically adsorbed to negative charges of organic matter or the formation of sphere complexes external to the solid phase.

Exchangeable aluminum (Al^{3+}) content had no marked variation along the topolithosequence, with low values recorded in all profiles, mainly in the A horizon and increasing in depth. In addition, the potential acidity (H^+ and Al^{3+}) values were high and increase in depth along the topolithosequence (Table 2). Possibly, the intense rainy season of the region associated with unimpeded drainage would be the determining climate factors to acidify the soil in depth (Campos et al., 2012).

Along the topolithosequence, organic carbon (OC) contents were very higher in the surface horizons because of the concentration of organic matter from the decomposition of native vegetation (Santos et al., 2012). Cation exchange capacity (CEC) ranged from high to very high, with values between 12 and 28 $cmol_c\ dm^{-3}$. The same trend occurred for the sum of bases (SB), which was higher in the A horizon mainly because of the OM and low clay content, which had low activity.

Due to the low activity of the clay fraction, all segments were classified as dystrophic (Table 2). This evidence is a result of the depletion of bases (Ca^{2+}, Mg^{2+}, and K^+), which is in accordance with other investigations developed in the Amazon region (CAMPOS et al., 2012ab; Santos et al., 2012; Martins et al., 2006). This is an interesting aspect since it evidences the Amazon conditions related to the constitution of formation of the parent material associated with weathering conditions of climate, leading the values of base saturation to present a gradient coincident with the geomorphic surfaces, being dystrophic along the topolithosequence. This result is different from those found by Campos et al. (2010), who observed a higher degree of soil development at top positions and dominance of dystrophic soils.

Soils were considered alic along the topolithosequence, with values of aluminum saturation (m) ranging from 51 to 91%. Martins et al. (2006) studied soils in a transition fields-forest in the region of Humaitá, AM, and also reported the percentage magnitude found here. This is an inherent characteristic of the sandstone-gneiss, which has by nature an acidic character. The richness in Al justifies the formation of gibbsite in the Neosols (upper and lower third), as mentioned.

https://doi.org/10.5194/se-2019-131
Preprint. Discussion started: 3 September 2019

Available phosphorus (P) contents showed a similar behavior along the topolithosequence, with an average of 2.0 mg kg^{-1} and decreasing in depth. Silva et al. (2006) stated that P remains stable in depth due to its low mobility. Another point considered is the strong affinity of iron oxides, mainly goethite in phosphorus retention (Pinto et al., 2013; Rotta et al., 2015). Goethite soils, as is our study, have their P adsorption affinity potentiated because of the high isomorphic substitution (IS) and SSA of Gt. However, the positions at the top and transport and deposition foothills presented values of 4.6 and 5.8 mg kg^{-1}, respectively, of available phosphorus in the A horizon, with the highest values in the topolithosequence. This would be an effect of OM accumulation in the form of litter on the soil surface horizon. In addition, OM acts as a physical barrier, inhibiting the direct contact of P to the soil active sites, thus allowing P in the available soil fraction (Fink et al., 2014).

4.4 Mineralogical attributes

The mineralogy of the clay fraction (Table 3) of diagnostic and transitional B horizons showed the coexistence of the minerals kaolinite (Kt), gibbsite (Gb), hematite (Hm), and goethite (Gt). In a preferred order, Fe oxides, Hm, and Gt predominate as follows: transport foothill (9–41g kg^{-1}) > deposition foothill (5–39 g kg^{-1}) > top (5–24 g kg^{-1}) > upper and lower third (1–5 g kg^{-1}). Among the iron oxides, Gt participated in the clay fraction of all studied soils, which is due to the iron poverty of sandstone-gneiss sediments (Correa et al., 2008; Santos et al., 2010). Under this lithological condition, Gt preferably has its formation favored (Barrón and Torrent, 2002; Viscarra Rossel et al., 2010), as shown by the low Hm contents, with a maximum value of 9 g kg^{-1} in the topolithosequence.

TABLE 3. Crystallographic attributes of soil minerals of a topolithosequence in Amazonas, Brazil.

Soil	MCD				WHH		SSA		IS		Ratio	Content	
	°2θ						$m^2\ g^{-1}$		mol mol^{-1}			g kg^{-1}	
	Gt_{110}	Gt_{111}	Hm_{110}	Hm_{012}	Kt	Gb	Gt	Hm	Gt	Hm	Kt/(Kt+Gb)	Gt	Hm
CXvd_AB	20.6	9.4	21.6	31.1	0.5	0.25	116.3	54.4	0.43	0.07	0.56	24	5
CXvd_Bi	15.2	8.9	16.4	54.6	0.51	0.31	159.7	79.9	0.15	0.02	0.45	21	5
RRd_ACr	25.1	18.2	25.4	28.3	0.50	0.17	94.6	41.3	0.38	0.04	0.87	5	1
RQo_Cr	25.1	13.9	12.8	36.6	0.70	0.28	94.6	89.4	0.33	0.02	0.76	5	1
FTd_Bf	18.5	14.9	22.8	30.2	ni	0.34	130.1	47.2	0.39	0.12	0.37	41	9
FTd_BAf	10.4	7.8	15.0	89.6	0.48	0.30	234.3	78.6	0.31	0.11	0.41	40	9
PAd_Bf	23.7	11.9	13.9	63.0	0.55	0.28	100.5	77.5	0.36	0.17	0.63	39	9
PAd_Btf	28.4	21.2	17.7	49.1	0.50	0.27	82.93	63.5	0.44	0.13	0.60	25	5

MCD: mean crystal diameter; WHH: width at half-height, SSA: specific surface area, IS: isomorphic substitution; Gt:goethite; Hm: hematite; Kt: kaolinite; Gb: gibbsite; ni: not identified.

https://doi.org/10.5194/se-2019-131
Preprint. Discussion started: 3 September 2019

Solid Earth Discussions

365 In general, the crystallographic parameters (MCD, WHH, SSA, and IS) were sensitive to the peculiarities of
366 the topolithosequence (Table 3). The mean crystal diameter (MCD) values for Gt110 (10–28 nm) and Gt111
367 (9–21 nm) peaks lower than Hm111 (12–25 nm) and Hm012 (30–89 nm) peaks revealed the persistence of the
368 crystalline Hm in relation to Gt, a common characteristic in tropical soils (Inda Júnior and Kämpf, 2005;
369 Barbieri *et al*., 2014) clearly observed in the transport foothill, where peaks referring to the face of Hm012 are
370 well-defined and narrow (Figure 4). The climatic conditions of the Amazon, especially precipitation and
371 temperature, combined with the natural increase of OM, acid pH (Table 2), and intense microbial activity,
372 contribute to a higher presence of Al in the goethite structure, which decreases its crystallinity.

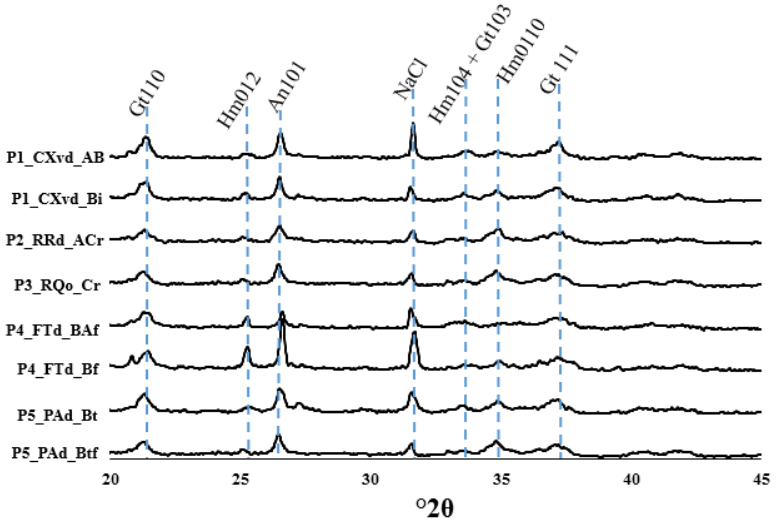

373

374 Figure 4. X-ray diffractograms of the clay fraction for hematite (Hm) and goethite (Gt) in the profiles of Haplic
375 Cambisol (CXvd_AB), Regolithic Neosol (RRd_ACr), Quartzarenic Neosol (RQod_Cr), Argiluvic Plinthosol
376 (FTd_Bf; P4_FTd_BAf), and Yellow Argisol (PAd_Bt; P5_PAd_Btf) in Amazonas, Brazil.

377 Except for the top position, values of isomorphic substitution (IS) higher than 0.33 mol mol^{-1}, regardless of
378 the soil position in the topolithosequence, indicate soils with a markedly weathering, non-hydromorphic, and
379 acid pH (high Al activity) (Table 2). These conditions justify the persistence of Gt with a high Fe substitution
380 (r=0.065) by Al (r=0.053), which promoted the contraction of the unit cell and, consequently, increased the
381 specific surface area (SSA), ranging from 82 to 234 m^2 g^{-1} in Gt and 41 to 89 m^2 g^{-1} in Hm. These results are
382 consistent with those found by other authors in Brazilian soils (Melo et al., 2001; Correa et al., 2008; Carvalho

https://doi.org/10.5194/se-2019-131
Preprint. Discussion started: 3 September 2019

Filho et al., 2015) since the highest values of IS and SSA in Gt are attributed to its higher structural capacity to accommodate Al in relation to Hm (Schwertmann and Taylor, 1989; Rolim Neto et al., 2004).

The contents of Fe oxides are concentrated in the soils in the following order: transport foothill > deposition foothill > top > upper and lower third (Table 3 and Figure 4). In turn, the highest contents of Fe oxide, especially Hm in the Plinthosol (P4), are due to an increase of iron in the BAf and Bf horizons, characterized by the presence of ferruginous concretions, which is peculiar to Plinthosols in the study region (Campos et al., 2012). Well-formed peaks of Gt were observed even in poorly developed profiles, as in the case of RQo_Cr, in which the presence of lytic contact (weak rock or outcropping saprolite) is noticeable (Figure 4). This fact was already expected since goethite is the first Fe oxide formed in the early stages of pedogenesis in the initial horizons close to the rock (Curi and Franzmeier, 1984; Silva, 2016).

The Kt/(Kt+Gb) ratio showed that Gb is an important constituent of the mineralogical assembly of the studied soils, except for upper and lower thirds and deposition foothill (Table 1 and Figure 5). The lower Kt contents, as well as its absence in the transport foothill, are probably due to the higher iron oxides contents, which may have disrupted Kt nucleation, a behavior also observed in the studies of Gidhin et al. (2006). This resulted in the highest values of width at half-height (WHH), which ranged from 0.483 to 0.703 nm when compared to Gb crystals, which in turn ranged from 0.273 to 0.307 nm. This result indicates that Gb crystals are much more crystalline than Kt, which is soil characteristic with a higher degree of weathering (Gidhin et al., 2006; Camargo et al., 2008), in which the growth of Gb crystals are favored by the low Si concentration in the soil (HSU, 1989).

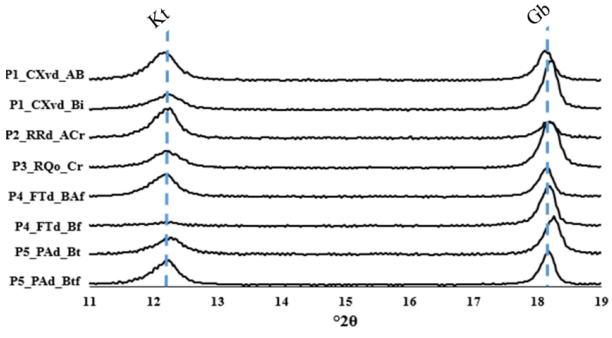

Figure 5. X-ray diffractograms of the clay fraction for kaolinite (Kt) and gibbsite (Gb) in the profiles of Haplic Cambisol (CXvd_AB), Regolithic Neosol (RRd_ACr), Quartzarenic Neosol (RQod_Cr), Argiluvic Plinthosol

https://doi.org/10.5194/se-2019-131
Preprint. Discussion started: 3 September 2019

(FTd_Bf; P4_FTd_BAf), and Yellow Argisol (PAd_Bt; P5_PAd_Btf) in Amazonas, Brazil.

The proportions of Kt[Kt/Kt+Gb > 75], associated with the low iron oxide contents found in Neosol profiles, confirm the lower intensity of pedogenesis or that morphogenesis predominated over the pedogenesis (Scarciglia et al., 2005). Thus, the geomorphological characteristics such as a more rugged and dissected topography of Neosol environments (Figure 3) favored the partial removal of basic cations and silicon, which are combined in the soil to form Kt (Kämpf et al., 2009). In addition, part of this Si and Al removed from the weathering of soils located at the landscape top could have been transported and accumulated in the lower landscape positions, which increased the values of the Kt[Kt/Kt+Gb > 60] ratio in Argisols (P5). These evidences are in accordance with several studies (Curi and Franzmeier, 1984; Ghidin et al.. 2006; Campos et al., 2007; Silva, 2016), which considered the landscape a passive factor of formation and retribution of pedogenic minerals.

5 Conclusions

Landscape separation into compartments and parent material identification were efficient for understanding the variation of soil attributes along the transect.

Variations in soil classes are related to topography surfaces and parent material, thus showing variations related to physical, chemical, morphological, and mineralogical attributes.

The mineralogy of the clay fraction is composed of kaolinite, goethite, hematite, and gibbsite, with goethite being the predominant iron oxide. In addition, mineralogy confirmed that the chemical properties, especially the cations of exchangeable bases, from sediments originating from these soils were naturally poor in bases and, therefore, not related to the removal process of the system, as it is widely recognized in the Amazon region.

A sand fraction dominance was observed in relation to the other fractions in all the surfaces, which is related to the alluvial nature of the parent material, with the highest values occurring in the Quartzarenic Neosol and increasing values as soil profile deepens.

Acknowledgment

Conselho Nacional de Desenvolvimento Científico e Tecnológico (CNPq), Coordenação de Aperfeiçoamento de Pessoal de Nível Superior (CAPES), Fundação de Amparo à Pesquisa no Estado do Amazonas (FAPEAM).

References

https://doi.org/10.5194/se-2019-131
Preprint. Discussion started: 3 September 2019

Barbieri D. M., Marques Júnior J., Siqueira D.S., Teixeira D.B., Panosso A.R., Pereira G.T., La Scala Junior N. Iron oxides and quality of organic matter in sugarcane harvesting systems. Revista Brasileira de Ciência do Solo. 38, 1143-1152. http://dx.doi.org/10.1590/S0100-06832014000400010, 2014.

Barrón V., Torrent J. Evidence for a simple pathway to maghemite in earth and mars soils. Geochimica et Cosmochimica Acta, 66, 2801-2806. https://doi.org/10.1016/S0016-7037(02)00876-1, 2002.

Bockheim J.G., Gennadiyev N.A., Hammer R.D., Tandarich J.P. Historical development of key concepts in pedology. Geoderma. 124, 23-36. https://doi.org/10.1016/j.geoderma.2004.03.004, 2005.

BRASIL. Ministério das Minas e Energia. Projeto Radam Brasil. Brasil: 1978.

Camargo L.A., Marques J.R.J., Pereira G.T., Horvat R. Variabilidade espacial de atributos mineralógicos de um Latossolo sob diferentes formas do relevo. I - Mineralogia da fração argila. Revista Brasileira de Ciência do Solo. 32, 2269–2277. http://dx.doi.org/10.1590/S0100-06832008000600006, 2008.

Campos M.C.C. Relações solo-paisagem: conceitos, evolução e aplicações. **Ambiência**, 8: 963-982. doi:10.5777/ambiencia.2012.05.01rb, 2012c.

Campos M.C.C., Ribeiro M.R., Souza Júnior V.S., Ribeiro Filho M.R., Almeida M.V. Revista Brasileira de Ciência do Solo. 36: 325 – 336, 2012b.

Campos M.C.C., Marques Júnior J., Pereira G.T., Montanari R., Camargo L.A. Relações solo-paisagem em uma litossequência arenito-basalto na região de Pereira Barreto, SP. Revista Brasileira de Ciência do Solo. 31, 519-529, 2007.

Campos M.C.C., Ribeiro M.R., Souza Júnior V.S., Ribeiro Filho M.R., Costa E.U.C. Segmentos de vertente e atributos do solo de uma topossequência na região de Manicoré, AM. Revista Ciência Agronômica. 41, 501-510, 2010.

Campos M.C.C., Ribeiro M.R., Souza Júnior V.S., Ribeiro Filho M.R., Souza R.V.C. Relações solo-paisagem em uma topossequência sobre substrato granítico em Santo Antônio do Matupi, Manicoré (AM). Revista Brasileira de Ciência do Solo. 35, 13-23. http://dx.doi.org/10.1590/S0100-06832011000100002, 2011.

Campos M.C.C., Ribeiro M.R., Souza Júnior V.S., Ribeiro Filho M.R., Souza R.V.C.C., Almeida M.C. Topossequência de solos na transição Campos Naturais-Floresta na região de Humaitá, Amazonas. Acta Amazônica. 42, 387-398. http://dx.doi.org/10.1590/S0044-59672012000300011, 2012a.

Carvalho Filho A., Inda Júnior A.V., Fink J.R., Curi N. Iron oxides in soils of different lithological origins in

https://doi.org/10.5194/se-2019-131
Preprint. Discussion started: 3 September 2019

461 Ferriferous Quadrilateral (Minas Gerais, Brazil). Applied Clay Science. 118, 1–75.
462 https://doi.org/10.1016/j.clay.2015.08.037, 2015.
463 Correa M.M., Ker J.C., Barrón V., Fontes M.P.F., Torrent J., Curi N. Caracterização de óxidos de ferro de
464 solos do ambiente tabuleiros costeiros. Revista Brasileira de Ciência do Solo. 32, 1017-1031.
465 http://dx.doi.org/10.1590/S0100-06832008000300011, 2008.
466 CPRM, Serviço Geológico do Brasil. Centro de Pesquisa de Recursos Minerais. Hidroclimatologia, geologia,
467 recursos minerais, geomorfologia e unidades de paisagens. Relatório Técnico. Manaus: 2001.
468 Curi N., Franzmeier D.P. Toposequence of Oxisols from the Central Plateau of Brazil. Soil Science Society
469 America Journal. 48, 341- 346. doi:10.2136/sssaj1984.03615995004800020024x, 1984.
470 Dalamerlinda E.A., Souza Júnior V.S., Wadt P.G.S., Deng Y., Campos M.C.C., Câmara, E.R.G. Soil-
471 landscape relationship in a chronosequence of the middle Madeira River in southwestern Amazon, Brazil.
472 Catena. 149: 199-208. https://doi.org/10.1016/j.catena.2016.09.021, 2017.
473 Dalrymple J.B., Blong R.J., Conacher A.J. A hypothetical nine unit landsurface model. Z. Geomorphology.
474 12, 60-76, 1968.
475 Donagema G.K., Campos D.V.B., Calderano S.B., Teixeira W.G., Viana J.H.M. Manual de métodos de análise
476 de solo. 3nd ed. Rio de Janeiro: Embrapa Solos, 2017.
477 Fink J.R., Inda A.V., Bayer C., Torrent J., Barrón V. Mineralogy and phosphorus adsorption in soils of south
478 and central-west Brazil under conventional and no-tillage systems. Acta Science Agronomic. 36, 379–387.
479 http://dx.doi.org/10.4025/actasciagron.v36i3.17937, 2014.
480 Ghidin A.A., Melo V.F., Lima V.C., Lima J.M.J.C. Topossequências de latossolos originados de rochas
481 basálticas no paraná. I – Mineralogia da fração argila. Revista Brasileira Ciência Solo. 30, 293-306.
482 http://dx.doi.org/10.1590/S0100-06832006000200010, 2006.
483 Hsu P.H., Dixon J.B., Weed S.B. In: Aluminiun oxides and oxyhydroxides. eds. Minerals in soil environments.
484 2nd ed. Madison; Soil Science Society of America: 331- 378. 1989.
485 Inda Júnior A.V, Kämpf N. Variability of goethite and hematite via reductive dissolution in soils of the tropical
486 and subtropical. Revista Brasileira Ciência Solo. 29, 851-866. http://dx.doi.org/10.1590/S0100-
487 06832005000600003, 2005.
488 Kämpf N. Die Eisenoxidmineralogie einer Klimasequenz von Böden aus Eruptiva in Rio Grande do Sul,

https://doi.org/10.5194/se-2019-131
Preprint. Discussion started: 3 September 2019

Brasilien. Doctoral thesis. Freising, Technische Universitat München, Munique, 1981.

Kämpf N, Curi N, Marques J.J. Óxidos de alumínio, silício, manganês e titânio. In: Melo, V.F. and Alleoni L.R.F. Química e mineralogia do solo. Viçosa: Sociedade Brasileira de Ciência do Solo, 2000.

Kämpf N, Curi N. Tópicos em ciência do solo - óxidos de ferro: Indicadores de ambientes pedogênicos e geoquímicos. Viçosa: Sociedade Brasileira de Ciência do Solo, 2000.

Klug H.P., Alexander L.E. X-Ray Diffraction Procedures for Polycrystalline and Amorphous Materials. New York: Wiley, 1974.

Kroth P.L. Disponibilidade de fósforo no solo para plantas e fatores que afetam a extração por resina de troca em membrana. Universidade Federal do Rio Grande do Sul, Porto Alegre, 1988.

Li Z.W., Zhang G.H., Geng R., Wang H. Rill erodibility as influenced by soil and land use in a small watershed of the loess plateau, China. Biosystems Engineering. 129, 248-257. https://doi.org/10.1016/j.biosystemseng.2014.11.002, 2015.

Marques Júnior J., Lepsch I.F. Depósitos superficiais neocenozóicos, superfícies geomórficas e solos em Monte Alto, SP. Geociências. 19, 90-106, 2000.

Martins G.C., Ferreira M.M., Curi M., Vitorino A.C.T., Silva M.L.N. Campos nativos e matas adjacentes da região de Humaitá (AM): atributos diferencias dos solos. Ciência e Agrotecnologia. 30, 221-227. http://dx.doi.org/10.1590/S1413-70542006000200005, 2006.

Mehra O.P., Jackson M.L. Iron oxide removal from soils and clays by a dithionite-citrate system buffered with sodium bicarbonate. In: Swineford A. National conference on clays and clay mineral. Pergamon Press, Washington, 317–342. https://doi.org/10.1016/B978-0-08-009235-5.50026-7, 1960.

Melo V.F, Fontes M.P.F., Novais R.F., Singh B., Schaefer C.E.G.R. Caracterização dos óxidos de ferro e de alumínio de diferentes classes de solos. Revista Brasileira de Ciência do Solo. 25, 19-32. http://dx.doi.org/10.1590/S01000683200100010003, 2001.

Minasny B., Mcbratney A.B. Mechanistic soil-landscape modelling as an approach to developing pedogenetic classifications. Geoderma. 133, 138-149. https://doi.org/10.1016/j.geoderma.2006.03.042, 2006.

Montanari R., Marques Júnior J., Campos M.C.C., Souza Z.M., Camargo L.A. Caracterização mineralógica de Latossolos em diferentes feições do relevo na região de Jaboticabal, SP. Revista Ciência Agronômica. 41, 191-199, 2010.

https://doi.org/10.5194/se-2019-131
Preprint. Discussion started: 3 September 2019

517 Murphy J., Riley J.P.A. Modified single solution method for the determination of phosphate in natural waters.
518 Anal Chimica Acta. 27, 31-36. https://doi.org/10.1016/S0003-2670(00)88444-5, 1972.
519 Neves, C.M.N., Silva, M.L.N., Curi, N., Macedo, R.L.G., Moreira, F.M.S., Norrish K., Taylor R.M. The
520 isomorphous replacement of iron by aluminum in soil goethites. Journal Soil Science. 12, 294–306.
521 https://doi.org/10.1111/j.1365-2389.1961.tb00919.x, 1961.
522 Pinto F.A., Souza E.D., Paulino H.B., Curi N., Carneiro M.A.C.P.: P-sorption and desorption in Savanna
523 Brazilian soils as a support for phosphorus fertilizer management. Ciência e Agrotecnologia. 37, 521-530.
524 http://dx.doi.org/10.1590/S1413-70542013000600005, 2013.
525 Ribeiro M.R., Oliveira L.B., Araujo Filho J.C., Ker J.C., Curi N., Schaefer C.E.G.R., Vidal-Tornado P.
526 Caracterização Morfológica do solo. eds. Pedologia; fundamentos, 2012.
527 Rotta L.R., Paulino H.B., Anghinoni I., Souza E.D., Carneiro M.A.C. Phosphorus fractions and availability in
528 a haplic plinthosol under no-tillage system in the brazilian cerrado. Ciência e Agrotecnologia. 39, 216-224.
529 http://dx.doi.org/10.1590/S1413-70542015000300002, 2015.
530 Santos A.C., Pereira M.G., Anjos L.H.C., Bernini T.A., Cooper M., Nummer A.R., Francelino M.R. Gênese e
531 classificação de solos numa topossequência no ambiente de mar de morros do médio Vale do Paraíba do Sul,
532 RJ. Revista Brasileira de Ciência do Solo**.** 34, 1297-1314. http://dx.doi.org/10.1590/S0100-
533 06832010000400027, 2010.
534 Santos H.G., Jacomine P.K.T., Anjos L.H.C., Oliveira V., Lumberas J.F., Coelho M.R., Almeida J.A., Cunha
535 T.J.F., Oliveira J.B. Centro Nacional de Pesquisa de Solos. Sistema Brasileiro de Classificação de Solos**.**
536 Brasília, 353p, 2013.
537 Santos L.A.C., Campos M.C.C., Costa H.S., Pereira A.R.: Caracterização de solos em uma topossequência
538 sob terraços aluviais na região do médio rio Madeira (AM). Ambiência - Revista do Setor de Ciências Agrárias
539 e Ambientais**.** 8, 319-331. doi:10.5777/ambiencia.2012.02.07, 2012.
540 Santos R.D., Lemos R.C., Santos H.G., Ker J.C., Anjos L.H.C., Shimizu S.H.: Manual de descrição e coleta
541 de solos no campo. 6nd ed. Viçosa: Sociedade Brasileira de Ciência do Solo, 2013.
542 Scarciglia F., Pera E., Critelli S.: Weathering and pedogenesis in the Sila Grande Massif (Calabria, South
543 Italy): from field scale to micromorphology. Catena. 61, 1–29. https://doi.org/10.1016/j.catena.2005.02.00,
544 2005.

https://doi.org/10.5194/se-2019-131
Preprint. Discussion started: 3 September 2019

Schiavo J.A., Pereira M.G., Miranda L.P.M.D., Neto D., Hypólitom A., Fontana A.: Caracterização e classificação de solos desenvolvidos de arenitos da formação Aquidauana-MS. Revista Brasileira de Ciência do Solo. 3, 881-889. http://dx.doi.org/10.1590/S0100-06832010000300029, 2010.

Schulze D.G., Schwertmann U.: The influence of aluminium on iron oxides: X. Properties of Al-substituted goethites. Clay Miner. 19, 521–539. https://doi.org/10.1180/claymin.1984.019.4.02, 1984.

Schwertmann U., Kampf N.: The effect of environments on iron oxide minerals. Advances Soil Science. 1, 172–200, 1985,

Schwertmann U., Taylor R.M.: Iron oxides. In: Dixon JB, Weed SB. Minerals in soil environments. 2nd ed. Soil Science Society of America, Madison, 379–438, 1989.

~~Silva L. S.: Mineralogia da fração argila dos solos do Planalto Ocidental Paulista [dissertação]. Jaboticabal: Faculdade de Ciências Agrárias e Veterinária, Universidade Estadual Paulista (UNESP), 2006.~~

Silva M.B., Anjos L.H.C., Pereira M.G., Nascimento R.A.M. Estudo de toposseqüência da baixada litorânea fluminense: Efeitos do material de origem e posição topográfica. Revista Brasileira Ciência Solo. 25, 965-976. http://dx.doi.org/10.1590/S0100-06832001000400019, 2001.

Skogley O., Dobermann A. Synthetic Ion-exchange Resins: Soil and envinonmental studies. Journal of Enviromental Quality. 25, 13-24. doi: 10.2134/jeq1996.00472425002500010004x, 1996.

Sommer M.: Influence of soil pattern on matter transport in and from terrestrial biogeosystems - A new concept for landscape pedology. Geoderma. 133; 107–123. doi: 10.1016/j.geoderma.2006.03.040, 2006.

Vasconcelos V., Carvalho Júnior A.O., Martins E.S., Couto Júnior A.F., Guimaraes R.F., Gomes R.A.T.; Sistema de classificação geomorfométrica baseada em uma arquitetura sequencial em duas etapas: árvore de decisão e classificador espectral, no Parque Nacional da Serra da Canastra. Revista Brasileira Geomorforfologia. 13, 171–186, 2012.

Rossel R.A.V., Rizzo R., Dematte J.A.M., Behrens T.: Spatial modeling of a soil fertility index using visible-near-infrared spectra and terrain atributes. Soil Science Society of America Journal. 74, 1293-130. doi: 10.2136/sssaj2009.0130, 2010.

ZEE - Zoneamento Ecológico Econômico Do Sul-Sudeste Do Amazonas, Am. (2008) Zoneamento Ecológico Econômico do Sul-Sudeste do Amazonas. Manaus: IPAAM.